Int. J. Electrochem. Sci., 17 **(2022)** Article Number: 22088, doi: 10.20964/2022.08.15

International Journal of
ELECTROCHEMICAL
SCIENCE
www.electrochemsci.org

Short Communication

Laser assisted synthesis of $Al_{0.1}CoCrFeNi$ High Entropy Alloy Coating: Microstructures and Properties

Xiaojing Wang[1], *Zhou Lan*[1], *Yanjie Liu*[2], *Ning Liu*[1,*], *Jiacheng Fan*[1], *Muye Niu*[1], *Yanxin Qiao*[1], *Bin Liu*[1]

[1] School of Materials Science and Engineering, Jiangsu University of Science and Technology, Zhenjiang, Jiangsu, 212003, P R China
[2] Materials Genome Institute, Shanghai University, Shanghai 200444, P. R. China
[*]E-mail: lnlynn@126.com, lynnliu@just.edu.cn

Received: 15 March 2022 / *Accepted:* 26 May 2022 / *Published:* 4 July 2022

In this work, $Al_{0.1}CoCrFeNi$ high-entropy alloy coatings were prepared by laser cladding on the surface of H13 steel, respectively by preset method and synchronous powder feeding method. Both the preset coating and synchronous coating show simple structure of FCC (Face-Centered Cubic) solid solution. Also, similar microstructures are obtained, which are typically fine equiaxed crystals at upper layer and columnar crystals with obvious growth trends near the metallurgical bonding interface of coating and matrix. Obvious passivation phenomenon can be observed in the potentiodynamic polarization curves. The coatings show larger corrosion potentials and lower corrosion current density that H13 steel, indicating that the coatings exhibit better corrosion performance than H13 steel. Furthermore, with the various loads, the coatings always show smaller the friction and wear coefficient and the volume wear rate than H13 steel. It indicates that H13 steel can be optimized by laser cladding $Al_{0.1}CoCrFeNi$ high-entropy alloy coatings.

Keywords: high-entropy alloys; microstructure; corrosion resistance; wear resistance

1. INTRODUCTION

H13 (4Cr5MoSiV1) steel is a commonly used material with high impact toughness, wear resistance, and ductility for die casting molds, hot forging and extrusion dies, The steel undergoes intense compression and abrasion, and for the corrosive atmosphere around the molds, corrosion destroy is another possible failure mode [1]. However, with the developing requirements in the field of die production, high precision quality and excellent performance are demanded. Currently, how to achieve the required performance of die production becomes one of the important researching subjects. Surface modification technique can be the answer. Laser surface forming technique is proved to be an effective

way, coatings with excellent properties can be fabricated by means of laser cladding due to its high heating/cooling rates and temperature gradient [2-5]. More recently, a damaged H13 steel die head was laser-coated with an AlCoCrFeNiTi high-entropy alloy and put into service, it shows that this repair method provides significant improvement in die head life [6].

HEAs (High-entropy alloys), composing of multi-principal elements, have attracted extensive attentions due to the promising performance [7-14]. Many previous researches show that high entropy coating can successfully improve the surface performance of various substrates, it means high entropy coating can be a novel application trend for HEAs [15-27]. Laser cladding was applied to form $Al_xCoCrCuFeNi$ (x = 1.0 - 2.0) HEA coatings, which exhibit higher hardness and excellent wear resistance at elevated temperature, as well as, a better corrosion resistance than 314L stainless steel [15]. It is investigated that Cu free $Al_xCoCrFeNi$ HEA coatings with various Al contents (x is 0.3, 0.6, and 0.85) undergo a structure transformation from FCC to FCC+BCC (Body-Centered Cubic) to BCC, which results in an increase of hardness [20-22]. The hardness of AlCoCrFeNi HEA coating is 3 times of that of 304 stainless steel, and the corrosion resistance performance was improved at the same time [23]. It is noteworthy that $AlCoCrFe_xNi$ (x = 1.5, 2.5) HEA coatings were improved by regulating the A2/B2 morphology, where A2 is Fe–Cr rich disordered BCC phase and B2 is Al–Ni rich ordered BCC phase [24]. Ni free AlCoCrCuFe HEA coating exhibits outstanding corrosion resistance in 1mol/L NaCl solution [25]. $Al_2CrFeCoCuTiNi_x$ HEA coatings with FCC + BCC structures show a maximum hardness up to 1102HV, which is about 4 times of the Q235 matrix, additionally, optical wear and corrosion resistances were achieved when x = 1 [26].

The above-mentioned HEA coatings always contained a high content of Al, however, the higher Al content can result in higher hardness and a tendency of crack. Until now, the effect of Al micro-alloying on HEA coatings did not concern. As is known, the dilution period can improve metallurgical bonding between the substrate and coating, and dilution rate can affect the microstructures and the properties of the coating. On the other, the microstructures and properties of coating can be influenced by different feeding ways and many process parameters, such as the laser power, the laser beam size, and the scanning velocity of the laser beam [5, 28-30].

Combining this information, the aim of this work is to provide a method to optimize the properties of H13 steel or provide an effective option for repairing of damaged dies. Herein, $Al_{0.1}CoCrFeNi$ (in atomic ratio) HEA coatings were fabricated by both preset method and synchronous powder feeding method respectively, optimal process parameters were obtained for both methods, and the microstructure and phase of the coatings were characterized, finally, wear and corrosion properties were assessed and compared with the H13 steel.

2. MATERIALS AND EXPERIMENT DETAILS

Prepared by gas atomization, $Al_{0.1}CoCrFeNi$ (in atomic ratio) HEA powders (originate from Shangdong province) with diameters in range of 150-200μm are used to fabricate high-entropy alloy coatings by means of preset method and synchronous powder feeding method respectively. As-received H13 steel in the forms of plate with diameter of 100mm and a thickness of 10mm was used as the

substrate material. The nominal chemical composition of H13 steel in wt. % is: C 0.45; Si 2.0; Mn 0.5; Cr 5.0; Mo 0.75; V 0.20; S ≤ 0.03; P ≤ 0.03 and Fe balance. The substrate plate was ground with 600 grade SiC paper to remove surface oxides or contaminants.

The $Al_{0.1}$CoCrFeNi HEA coatings were fabricated from spherical gas-atomized $Al_{0.1}$CoCrFeNi HEA powders. For preset cladding processing, the powder was mixed with polyvinyl alcohol and a small amount of alcohol to form paste, which can be paved in advance on the surface of H13 steel. Before laser cladding, the substrate was preheated for 2 h at 200˚C with $Al_{0.1}$CoCrFeNi HEA paste on it. For synchronous powder feeding processing, the powder was dried for 2 h at 200˚C before cladding and argon gas was introduced at a flow rate of 7 L/min coaxially from powder feeder (DPSF-2). Moreover, high purity argon gas at a flow rate 15 L/ min was used as shielding gas to prevent oxidation. Laser cladding was performed using a 6 kW Ytterbium-doped fiber laser (YLS-6000-S2T, IPG) equipped with a coaxial powder delivery nozzle (COAX-8, Fraunhofer IWS). The laser beam was focused into a 5 mm × 5 mm spot on the substrate, and the energy distributed uniformly in the laser spot. After a series of optimization trial runs, proper parameters were obtained and listed in Table 1.

Table 1. Proper parameters used in experiment

	laser power	scan rate	powder mass feed voltage
preset cladding processing	1.8 kW	1mm/s	-
synchronous powder feeding processing	1.2 kW	1mm/s	20V

The corrosion performance of the $Al_{0.1}$CoCrFeNi HEA coatings were studied with an electrochemical workstation (AUTOLAB, Switzerland). Friction-wear test was performed with ball-on-disk wear tester at room temperature. For comparison, the corrosion and wear resistance of H13 steel were also performed.

3. RESULTS AND DISCUSSION

The typical macro morphologies of the laser cladding $Al_{0.1}$CoCrFeNi HEA coatings are presented in Fig.1a. Clear metallurgical bonding interfaces can be seen between the substrate and coatings, and it is evident that the height of the preset coating is larger than that of the synchronous coating. The microstructures of both coatings are similar, as shown in Figs.1b and 1c, refined equiaxed grains were observed at the upper region of the cladding layer for the reason of compositional undercooling, while directional columnar crystals were found near metallurgical bonding interface as a result of the positive temperature gradient of liquid-solid interface. As illustrated in Table 2, the Fe content of the preset coating is 30.41%, which is lower than that of the synchronous coating, 34.05%. Correspondingly, the dilutions are 21.21% and 28.66% respectively for the preset and synchronous coatings. Both the preset and the synchronous coatings show FCC structure according to XRD (X-ray diffraction) results (Fig.2).

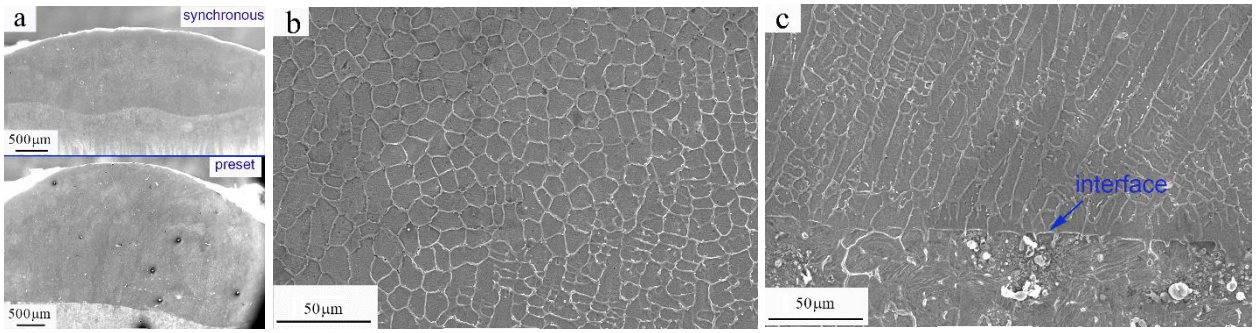

Figure 1 Images of $Al_{0.1}CoCrFeNi$ high-entropy alloy coating. (a) macro-profiles, (b) equiaxed crystals at the middle-upper part, (c) columnar crystals near the interface

Table 2 The compositions of the coatings (at. %)

samples	Fe	Cr	Ni	Co	Al
preset coating	30.41	25.48	21.89	19.77	2.45
synchronous coating	34.05	24.34	20.92	18.37	2.32

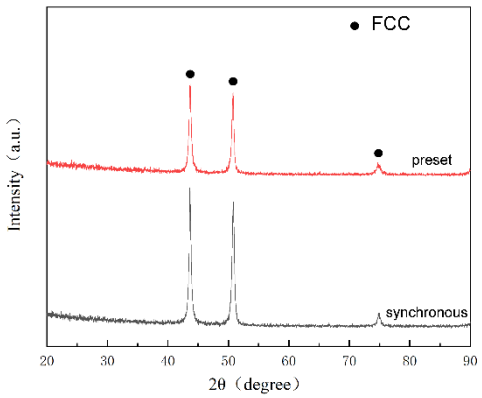

Figure 2 XRD patterns of $Al_{0.1}CoCrFeNi$ high-entropy alloy coatings

Fig.3a shows the potentiodynamic polarization curves of the coatings and H13 steel in the 3.5%NaCl solution at room temperature, wherein apparent passivation phenomenon can be seen, it means that protective oxidation layers were formed on the surface of the coatings and H13 steel in 3.5%NaCl solution. As is known, corrosion potential means the thermodynamics stability, that is, the possibility of occurrence of corrosion; while corrosion current density indicates the dynamics process of corrosion, i.e., the corrosion rate once corrosion occurs. In general, the higher corrosion potential (E_{corr}) and smaller corrosion current density (I_{corr}) refer to better anticorrosion properties. According to Table 3, it is evident that the coatings exhibit higher E_{corr} and smaller I_{corr} than H13 substrate. In addition, the critical pitting potential (E_{pit}) of the coatings is higher than that of H13 substrate, it means that, pitting corrosion is prone to occur on the surface of the H13 substrate in 3.5%NaCl solution, compared with the coatings. In summary, the corrosion resistance of the $Al_{0.1}CoCrFeNi$ HEA coating is superior to the H13 steel substrate in 3.5% NaCl solution. Moreover, the preset coating exhibits the maximum E_{corr} (-0.364V) and the minimum I_{corr} ($2.236\times10^{-7}\mu A/cm^2$), indicating the optimal corrosion resistance in this work.

Moreover, $Al_{0.1}CoCrFeNi$ HEA coatings prepared in this work exhibit a better corrosion resistance than some reported HEA coatings [31-37].

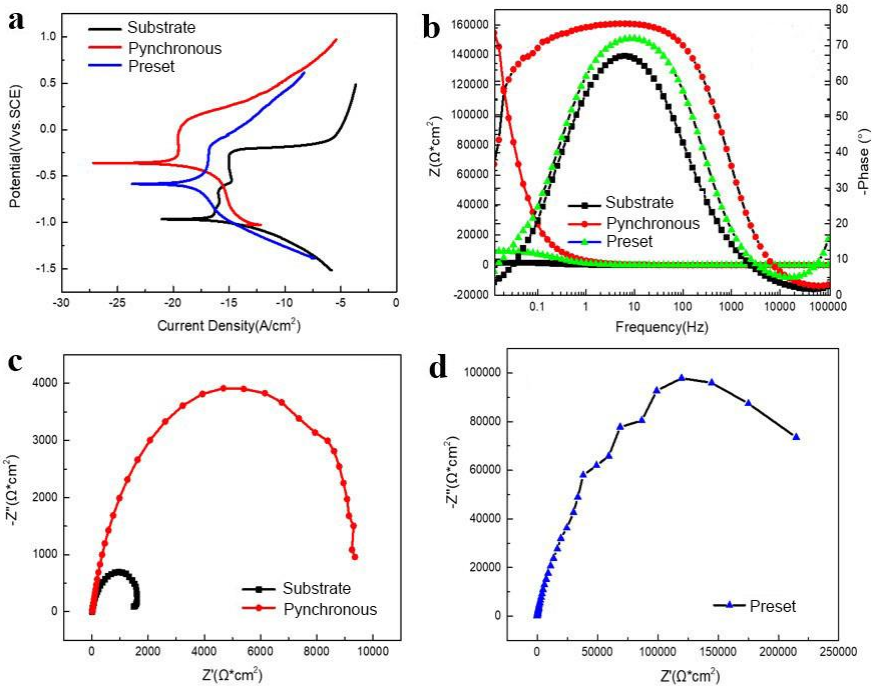

Figure 3 Potentiodynamic polarization curves (a), Nyquist diagram (b) and Bode diagram (c-d) of the coatings and substrate

Table 3 Electrochemical parameters of polarization test for coatings and substrates

	I_{corr} (A/cm^2)	E_{corr} (V)	
Preset coating	2.236×10^{-7}	-0.364	This work
Synchronous coating	5.498×10^{-7}	-0.586	This work
H13	6.664×10^{-6}	-1.017	This work
$CoCr_{2.5}FeNi_2$	3.648×10^{-5}	-0.714	[31]
AlFeCrCoNi	3.5×10^{-6}	-0.734	[32]
$Al_2FeCrCoNi$	6.3×10^{-7}	-0.58	[33]
$Al_2FeCrCoNiTi_{0.5}$	6.7×10^{-7}	-0.45	[33]
$Al_2FeCrCoCuTi$	6.8×10^{-5}	-0.51	[34]
FeCrCoCuNi	9.0×10^{-6}	-0.24	[35]
$Fe_{60}(CrCoNiTi)_{40}$	2.650×10^{-5}	-0.534	[36]
$FeCrCoCu_{1.5}Ni$	1.12×10^{-6}	-0.709	[37]

Electrochemical impedance spectroscopy was used to study the corrosion performance, and accordant results were shown in Fig. 3(b, c, d). According to Nyquist diagram in Fig.3b, the impedance values follow by the rank of the preset coating > the synchronous coating > H13 steel, indicating that better corrosion resistance can be achieved in $Al_{0.1}CoCrFeNi$ HEA coating. As shown in Fig.3c and 3d,

the radius of Bode curves of the coatings are quite larger than that of H13 steel, indicating that the coatings exhibit better corrosion resistance than H13 steel, and the preset coating is superior to the synchronous coating.

As shown in Fig.4a, the substrate always possess the largest friction coefficient under various loads, and the friction coefficient decrease with the increasing load. The wear weight loss of the worn coatings and substrate are shown in Fig.4b. With the increase of load, the wear weight loss increase as a result, and the substrate exhibits a considerable large increment. Relatively, at lower load, the difference of the wear weight loss between the coating and substrate is quite small, but dramatic difference can be found at the load of 15N. In summary, the wear resistance of the coatings is better than that of substrate, and the preset coating shows the superior wear resistance. On the one hand, for the reason of supersaturated solid solution caused by high entropy effect, the coating was strengthened, and on the other, the rapid solidified coating generated the microstructure refinement, which leads to the higher hardness of coating, and an excellent wear resistance as results. Compared with $CoCr_{2.5}FeNi_2$ HEA coatings [31,38-40], $Al_{0.1}CoCrFeNi$ HEA coatings prepared in this work exhibit a smaller volume wear rate.

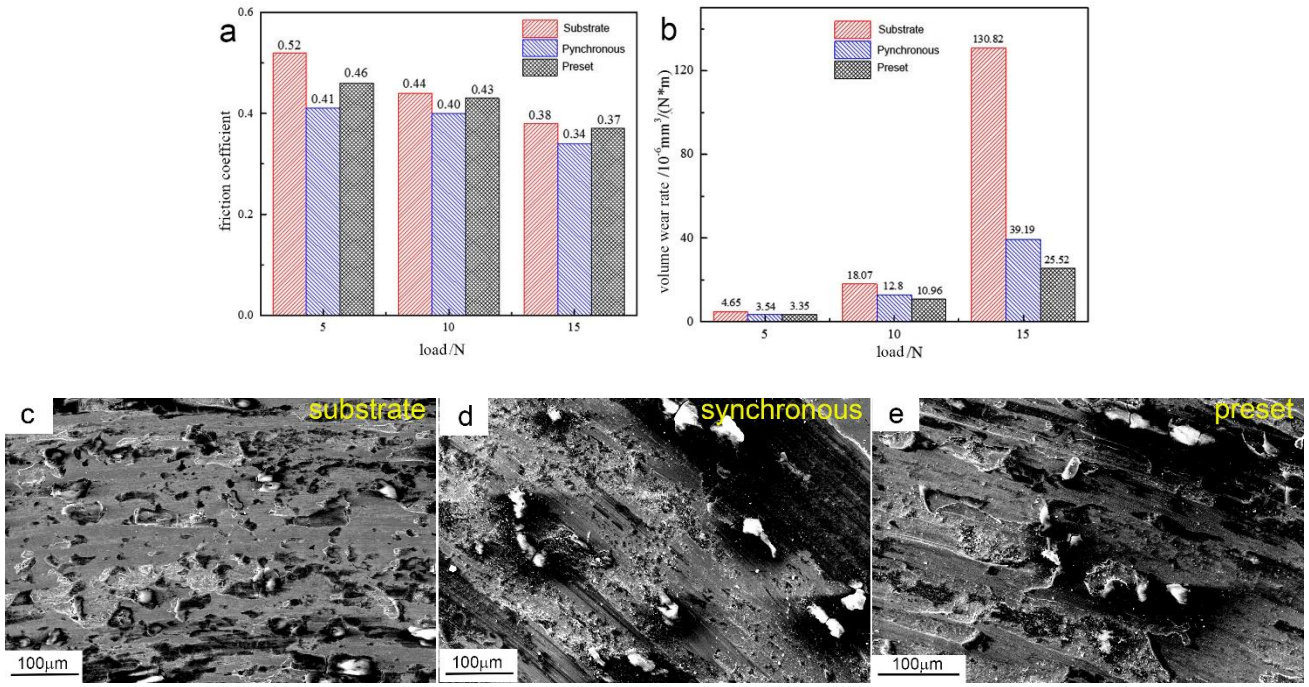

Figure 4. friction coefficient, volume wear rates and wear surface morphologies of the substrate and coatings (a) friction coefficient, (b) volume wear rates and (c-e) morphologies of the worn surfaces

Take the worn samples at the load of 15N for example, the morphologies of the worn surfaces were characterized by using SEM (Scanning Electronic Microscopy) and shown in Figs 4c-4d. A large amount of oxidation layers can be observed on the surface of the H13 substrate, accompanied by many pits. It indicates a mixture wear mechanism of oxidation wear, adhesive wear, and contact fatigue wear for substrate. While for the coatings, plastic deformation and abrasive dusts are found on the worn

surface, simultaneously, oxidation phenomenon can be observed in local area, it means that the wear mechanism involves adhesion, accompanied by oxidation wear.

4. CONCLUSIONS

(1) Similar microstructures were obtained in $Al_{0.1}CoCrFeNi$ HEA coatings by means of laser cladding at both preset and synchronous method. Metallurgical bonding between the substrate and coatings can be seen, and both the preset and the synchronous coatings show FCC structure.

(2) Obvious passivation phenomenon can be seen in the potentiodynamic polarization curves of the coatings and H13 steel in the 3.5%NaCl solution at room temperature. Good corrosion resistance can be achieved locally in H13 steel and a longer passivation can be seen, while critical pitting corrosion potential, E_{pit} is lower than that of the coatings. It indicates that passivation layer on the coatings are more protective than that on the H13 substrate. Moreover, the corrosion potential (E_{corr}) of the preset coating is higher than that of the synchronous coating and H13 substrate, accordingly, corrosion current density (I_{corr}) of the preset coating is lower than that of the synchronous coating and H13 steel, indicating that the preset coating shows a better corrosion resistance.

(3) The substrate always exhibits the largest friction coefficient under various loads. With the increasing load, the friction coefficients decrease, and the volume friction rates increase as results. The coatings show a cycle corrosion process of "oxidation - friction - exfoliation - oxidation", and substrate shows a serious mixture friction mechanism of "oxidation + adhesive + fatigue". In summary, the coatings always exhibit better wear resistance than the substrate at various loads.

CREDIT AUTHORSHIP CONTRIBUTION STATEMENT

Xiaojing Wang: Conceptualization, Methodology, Validation, Investigation, Writing – original manuscript, Writing – Original Draft & editing. Yanjie Liu: Conceptualization, Methodology, Validation, Investigation, Writing – review & editing. Ning Liu: Investigation, Writing – review & editing, Visualization. Jiacheng Fan: Data curation, Conceptualization, Supervision, Project administration, Funding acquisition, Writing – review & editing. Muye Niu: Wear related data analysis, Writing – review & editing. Yanxin Qiao: Corrosion related data analysis, Writing – review & editing. Bin liu: Project administration, Funding acquisition.

ACKNOWLEDGMENTS

This study was financially supported by the National Natural Science Foundation of China (NSFC), under the grant No. 51775254.

CONFLICTS OF INTEREST

The authors declare that they have no conflict of interest.

DATA AVAILABILITY:

The data used to support the findings of this study are available from the corresponding author upon request.

References

1. C. Zang, T. Zhou , H. Zhou, Y. Yuan, P. Zhang, L. Meng and C, Z. Zhang, *Opt. Laser Technol.,* 106 (2018)299.
2. D. Herzog, V. Seyda, E. Wycisk and A. Emmelmann, *Acta Mater.*, 117(2017)371
3. Y. Ding, C. Du, X. Wang, B. Zhang, *Adv. Compos. Hybrid Mater.*, 4(2021) 205
4. J.B. Cheng, Y. Feng, C. Yan, X.L. Hu; R.F. Li and X.B. Liang, *JOM*, 72(2020)745
5. R. M. Mahamood, Laser Metal Deposition Process of Metals, Alloys, and Composite Materials, Brian Derby, Manchester, UK
6. M. T. Wall, M. V. Pantawane, S. Joshi, F. Gantz, N. A. Ley, R.Mayer, A. Spires, M. L.Young and N. Dahotre, *Surf. & Coat. Technol.*, 387(2020)125473
7. B. Cantor, I. T. H. Chang, P. Knight and A. J. B. Vincent, *Mater. Sci. Eng. A*, 375-377 (2004) 213.
8. J. W. Yeh, S. K. Chen, J.Y.Gan, S.J.Lin, T.S.Chin, T.T.Shun, C.H.Tsau and S,Y.Chang. *Metall. Mater. Trans. A*, 35 (2004) 2533.
9. Y. Zhang, High-Entropy Materials: A Brief Introduction, Springer Nature Singapore Pte Ltd, 2019.
10. J.Y. He, H. Wang , H.L. Huang, X.D. Xu , M.W. Chen, Y. Wu, X.J. Liu, T.G. Nieh, K. An and Z.P. Lu, *Acta Mater.*, 102(2016)187.
11. P.H. Wu, N. Liu, W. Yang, Z. X. Zhu, Y.P. Lu and X.J. Wang, *Mater. Sci. Eng. A*, 642(2015)142.
12. S. Wang, Z. Chen, L.C. Feng, Y. Y. Liu, P. Zhang, Y.Z. He, Q.Q. Meng and J.Y. Zhang, *Mater. Charact.*, 144 (2018) 516.
13. M. Zhu, L.J. Yao, Y.Q. Liu, M. Zhang, K. Li and Z.Y. Jian, *Mater. Lett.,* 272 (2020) 127869.
14. N. Liu, W. Ding , Wang X J, J. Zhang, P.J.Zhou and C. Mu, *Mater. Sci. Technol.*, 36(2020)654.
15. Y.P. Lu, H. F. Huang, X. Z. Guo, C. L. Ren, J. Guo, H.Z. Zhang, S.J. Zheng, Q.Q. Jin, Y. H. Zhao, C.Y. Lu, T.M. Wang and T.J. Li, *J. Mater. Sci. Technol.*, 35(2019)369.
16. Q. X. Hu, X.L.Wang andJ.Y. Miao, *Coatings*, 11(2021)715.
17. Q. X. Hu, X.L.Wang and X. W. Shen, *Coatings*, 11(2021)1053.
18. L.H. Tian, M. Fu and W. Xiong, *Materials*,11(2018)320.
19. L.H. Tian, Z.K. Feng and W. Xiong, *Coatings*, 8(2018)112.
20. X.Y. Ye, M.X. Ma, Y.X.L. Cao, W. J. Liu, X.H. Ye and Y. Gu, *Phys. Procedi,* 12(2011) 303.
21. J. Joseph, T. Jarvis, X.H. Wu, N. Stanford and P. Hodgson, *Mater. Sci. & Eng., A* 633(2015)184.
22. J. Joseph, N. Stanford, P. Hodgson and D. M. Fabijanic, *J. Alloys Compd.,* 726 (2017)885.
23. Q.Chao, T. Guo, T. Javis, X. Wu, P. Hodgson and D. Fabijanic, *Surf. & Coat. Technol.*, 322(2017) 440.
24. M. Li, J.Gazquez, A.Borisevich, R.Mishra, K.M.Flores, *Intermetallics,* 95 (2018)110.
25. G.J. Zhang , Q.W. Tian , K.X. Yin, S.Q. Niu, M.H. Wu, W.W. Wang , Y.N. Wang and J.C. Huang , *Intermetallics*, 1195(2020)116722
26. S. Zhang, C.L.Wu, C.H. Zhang, M.Guan and J.Z.Tan, *Opt. Laser Technol.,* 84 (2016) 23.
27. X.W. Qiu, Y.P. Zhang, L. He and C.G. Liu, *J. Alloys Compd*., 549(2013)195.
28. X.W. Qiu and C.G. Liu, *J. Alloys Compd.,* 553(2013)216-220
29. Y. Yang and J.D.Hu, *Opt. Laser Technol.,* 43(2011)138.
30. S.A.Vaziri, H.R.Shahverdi and M.J. Torkamany, *Opt. Laser Technol.,* 47(2009)971.
31. Z. Gu, S. Xi and C. Sun, *J. Alloys Compd.,* 819(2013)152986.
32. Y. Shon, S. S. Joshi, S. Katakam, R. S. Rajamure and N. B. Dahotre, *Mater. Lett.,* 142 (2015) 122.
33. X.W. Qiu, *J. Alloys Compd.,*735(2018)359.
34. X. W. Qiu and C. G. Liu, *J. Alloys Compd.,* 553(2013)216.
35. X. W. Qiu, M. Wu, C. G. Liu, Y. Zhang and C. Huang, *J. Alloys Compd.,* 708(2017)353.
36. Z. Cai, X. Cui, G. Jin, Z. Liu, N. Tan, Y. Li and M. Dong, *Mater. Charact.*, 132 (2017) 373.
37. Y. Cai, Y. Chen, Z. Luo, F. Gao and L. Li, *Mater.Design,* 133(2017)91.
38. C. Huang, Y. Zhang, R. Vilar and J. Shen, *Mater.Design,* 41(2012)338.

39. M. Sha, L. Zhang, J. Zhang, N. Li, T. Li and N. Wang, *Rare Metal Mater. and Eng.*, 46(2017) 1237.
40. F.Y. Shu, L. Wu, H.Y. Zhao, S.H. Sui, L. Zhou, J. Zhang, W.X. He, P.He and B.S. Xu, *Mater. Lett.*, 211(2018) 235.